Korean J. Chem. Eng., 35(1), 147-152 (2018)
DOI: 10.1007/s11814-017-0245-4

pISSN: 0256-1115
eISSN: 1975-7220

Surface functionalized carbon microspheres for the recovery of copper ion from refinery wastewater

Subrata Mondal*,,†, Addisu Tadesse Derebe*, and Kean Wang*,*****

*Department of Chemical Engineering, The Petroleum Institute, Abu Dhabi, United Arab Emirates
**Department of Mechanical Engineering, National Institute of Technical Teachers' Training and Research (NITTTR) Kolkata, Sector III, Block FC, Salt Lake City, Kolkata 700106, West Bengal, India
***Department of Chemical Engineering, Khalifa University of Science & Technology, Abu Dhabi, United Arab Emirates
(*Received 14 March 2017 • accepted 6 September 2017*)

Abstract−Micro-sized carbon spheres (CNS) were synthesized by hydrothermal process from glucose solution at 443.15 K and two different reaction times. The synthesized CNS samples were surface functionalized with hydroxyl (-OH) functional groups using NaOH treatment, and were tested in batch adsorption to remove heavy metal ion (Cu^{2+}) from aqueous solutions. Experimental results revealed that CNS contains mostly amorphous carbon. NaOH functionalized CNS had significantly higher adsorption capacity of copper ~170×10^{-3} Kg Cu^{2+}/Kg-CNS as compared to the untreated CNS. The adsorption isotherms were well fitted by the Langmuir isotherm equation. The surface morphology of the native and functionalized CNS samples was characterized by a number of techniques and based on which the adsorption of copper ion was discussed.

Keywords: Adsorption, Carbon Microsphere, Heavy Metal Ions, Surface Functionalization, Water Treatment

INTRODUCTION

The rapid increases in population and industrialization processes have seriously contributed to highly toxic heavy metal pollution in our ecosystems. Various industries such as metal cleaning and plating baths, paper, paperboard mills, wood-pulp production, copper mine, tire manufacture, and fertilizer industries produce large amounts of solid and liquid waste containing toxic heavy metal ions: copper, silver, lead, nickel, mercury, etc. Discharge of these industrial effluents onto land and into the river increases the level of heavy metals in the environment and aquatic systems. Excessive intake of copper by humans results in its accumulation in the liver, leading to copper poisoning, e.g., gastrointestinal problems, miscarriages, and subtle abortions, while long-term exposure may cause liver and kidney damage, disorders of nervous system, as well as brain damage. According to ISI specifications, the discharge limits for Cu^{2+} in the effluents onto the land is 3.0 mg/L and above this concentration limit, the effluents must be treated before disposal [1,2].

The crude oil extraction and refining systems are accompanied by the production of large quantity of produced/process water, which may contain a high concentration of organics/salts/metal ions, etc. Table 1 presents partial analytical result of the process water from an oil terminal of the United Arab Emirates. In Table 1 the copper content is the highest among all metal ions. Such waste water with high content of organics and salts/ions seriously disturbs the local environment and should be treated before discharge into the environment.

Table 1. The chemical/metal content of the process water from an oil terminal

Test	Analytical method	Unit	Result
BOD	APHA 5210 B	mg/L	200
COD	APHA 5220 B	mg/L	850
Chlorine	APHA 4500 Cl^- B	mg/L	40,000
Salinity	Refractometry	%	7.2
Sulphur	APHA SO_4^{2-}	mg/L	2.2
Iron			5.6
Copper			**44**
Chromium	APHA 3219 B	mg/L	~0.1
Mercury			<0.01
Zinc			18

Physical and chemical treatment processes, such as coagulation, flotation, chemical precipitation, membrane filtration, and electrochemical methods are used to remove heavy metals from industrial effluents. However, these techniques have certain disadvantages, such as high capital investment and operational costs or the issues related with the treatment and disposal of the residual metal sludge. The adsorption process has been shown to be an alternative method for removing trace heavy metals from water and wastewater [3].

Carbon-based adsorbents are widely used to remove heavy metal from the industrial effluent [4-10]. Adsorption capacity of carbonaceous adsorbents depends on surface texture/chemistry. Often, surface modification of such materials is recognized as an attractive approach for enhancement of heavy metal removal. Different heavy metal ions have different affinities for different surface func-

†To whom correspondence should be addressed.
E-mail: subratamondal@yahoo.com

tional groups. Modifications can be performed by grafting specific functional groups onto the surfaces of adsorbent. It is well known that carbonaceous materials are able to effectively adsorb organic compounds in aqueous solutions. This chemical behavior leads to immobilization of organic compounds on the carbon surface [8]. Furthermore, modification of carbon adsorbents can enhance their natural ion exchange capability [11]. Aydın et al. reported several low cost adsorbents, such as shells of lentil (LS), wheat (WS), and rice (RS), for the removal of copper ions from the aqueous solution. The experimental study revealed that adsorbent derived from rice shell shows maximum adsorption capacity of 17.4×10^{-3} Kg/Kg of adsorbent at 313 K temperature [12]. Demiral and Güngör reported copper adsorption from the aqueous solution by using activated carbon derived from grape bagasse by chemical activation using phosphoric acid. The adsorbent showed maximum adsorption capacity of copper (II) of 43.47×10^{-3} Kg/Kg-adsorbent at 318.15 K [13]. Further, in addition to the conventional adsorbent, adsorptive membrane is also reported in the literature to recover copper ions from the aqueous solution [14]. Apart from copper removal, adsorbents were also used for the removal of other metal ions, such as adsorption of silver on activated carbon derived from coal, coconut shell and polyacrylonitrile have been reported by Jia et al. [15]. Bentonite clay was found an excellent adsorbent for silver adsorption, with the maximum capacity of 61.48×10^{-3} Kg-silver/Kg-adsorbent at 283 K [16]. Ozdes et al. presents removal of lead (Pb II) from aqueous solution by using waste mud which was activated with NaOH to enhance its adsorption capacity. Surface activated waste mud shows lead adsorption capacity of 24.4 * 10^{-3} Kg/Kg-adsorbent with a 10^{-2} Kg/L of surface functionalized waste mud concentration [17]. Biosorption procedure can also be used for the separation of heavy metal ions. Tuzen and Soylak reported nickel(II) and silver(I) at trace levels on *Bacillus sphaericus*-loaded Chromosorb 106 column [18].

Recently, there has been a significant research activity for the preparation of colloidal micro- and nano-sized spheres with specific intrinsic properties. By varying factors like chemical composition, crystallinity, diameter and bulk structure, the physical and chemical properties of the spheres can be tailored. Carbon microspheres contain C-OH and C=O groups, and the density of which can be further increased by treatment with a suitable reagent and the resulted micro-spheres presents excellent performance for the removal of metal ions from aqueous solutions. Song et al. shown that NaOH-treated CNS is an efficient adsorbent for the removal of dyes from aqueous solutions [19]. Frusteri et al. reported a simple and cost effective method for the preparation of CNS from the glucose solution by using hydrothermal reaction at 473.15 K. The obtained microspheres are 200-300 nm in size and amorphous with a surface area of ~600 m^2/g. Surface areas of microsphere can be increased after heat treatment in N_2 environment at 1,273.15 K. Further, CNS can be surface functionalized by using inorganic acid [20]. Frusteri et al. reported CNS prepared by pyrolysis of benzene at 1,173.15 K. The spheres were found to contain concentric and incompletely spherical graphitic sheet [21].

Heavy metals such as copper are hazardous not only to the environment but also to the biological species, and this has led to more stringent regulations on their discharge into the wastewater stream. Therefore, our objective was to develop an efficient and cost-effective adsorbent for the removal of copper from aqueous solution. Carbon microspheres (CNS) were synthesized by environmental friendly hydrothermal process and used as potential adsorbent for the recovery of copper.

EXPERIMENTAL

1. Materials

D-Glucose (>99% anhydrous), sodium hydroxide, acetic acid, silver nitrate and copper (II) nitrate trihydrate were obtained from Fisher Scientific. Deionized water was used for all experimental purposes.

2. Synthesis of CNS

Carbon microspheres (CNS) were synthesized using the method reported in the literature [22-24]. In brief, 40×10^{-3} L of 0.8 M glucose (D-Glucose, 99+%, anhydrous,) was loaded into a Teflon-lined autoclave (maximum capacity: 0.3 L, Series 4750, Parr Instrument Company, USA) and maintained at 443.15 K for 14 and 19 hrs. The obtained CNS microparticles were isolated from the aqueous solution by centrifugation. Afterwards, the CNSs were washed, and centrifuged in three cycles by deionized water and ethanol, respectively, before they were dried overnight in oven at 353.15 K.

3. Surface Activation of CNS

The native CNSs were treated with aqueous solutions of sodium hydroxide (NaOH) to enhance the density of hydroxyl groups on the surface. About 0.12×10^{-3} Kg of dry CNS powder was dispersed in 0.1 L of 0.5 M NaOH aqueous solution and stirred at 300 rpm for 1 h at room temperature. The surface-activated CNSs were collected by centrifugation and washed with deionized water (about 1 L) to remove the residual NaOH until the pH of the filtrate reached nearly neutral. Finally, the -OH functionalized CNS samples were dried in an oven at 353.15 K for 18 h and denoted as CNS-OH.

4. Characterizations of CNS

The morphology and surface characteristics of CNS samples were characterized by various characterization techniques. Fourier transform infrared (FTIR) spectra of all samples were obtained using a Bruker VERTEX 70 FTIR spectrometer. The samples were finely ground and pelletized together with KBr. For all samples the number of scans was set at 64 with a resolution of 4 cm^{-1}. Crystallographic order and disorder of CNS samples were studied by using Raman spectroscopy and transmission electron microscopy (TEM). CNS samples were characterized by using a Raman spectrometer (labRAM HR, Scientific - HORIBA, USA) in back scattering configuration at 633 nm laser wavelength. Surface morphology of CNS samples was studied by a scanning electron microscope (Quanta 250 FEG SEM, FEI, USA) at an accelerated voltage of 20 kV. The crystallographic structure of the CNSs was studied by an X-ray diffractometer (X'pert Pro MPD, PANalytical - X-ray diffractometers, USA), with a Cu-Kα radiation. Further, the surface area of the samples was determined by means of a nitrogen isotherm at 77 K using a pore and surface analyzer (Autosorb 6iSA, Quantachrome Instrument, USA). All samples were degassed for 8 hours at 423 K prior to N_2 adsorption tests to remove any residual water and/or organics.

5. Adsorption Studies

The adsorption of Cu^{2+} was measured on the native CNS and

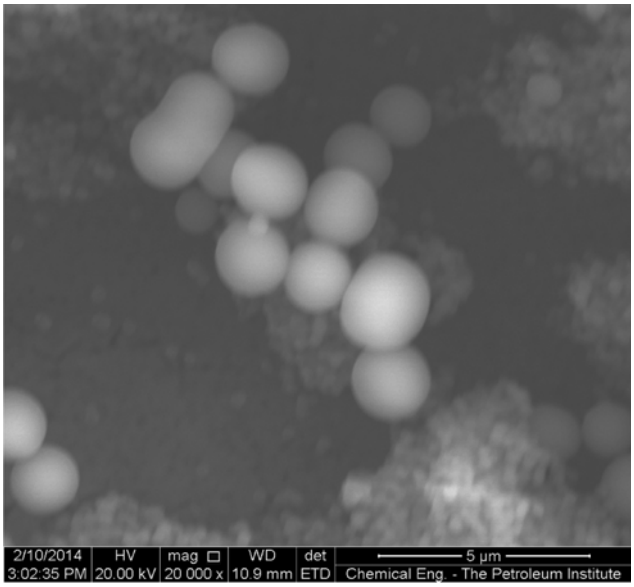

Fig. 1. SEM image of native CNS (reaction temperature: 170 °C, reaction time: 14 h).

surface activated CNS (CNS-OH) samples, in a series of batch experiments. About 25 mg of samples were added into 25 mL stock solution in a flask, and stirred at 250 rpm for 12 h at room temperature before being filtered out by a syringe filter of 0.2 µm pore size. The clear filtrate was then diluted in 2% HNO_3 for the analysis using an ICP-MS (PerkinElmer, SCIEX, ELAN DRC-e).

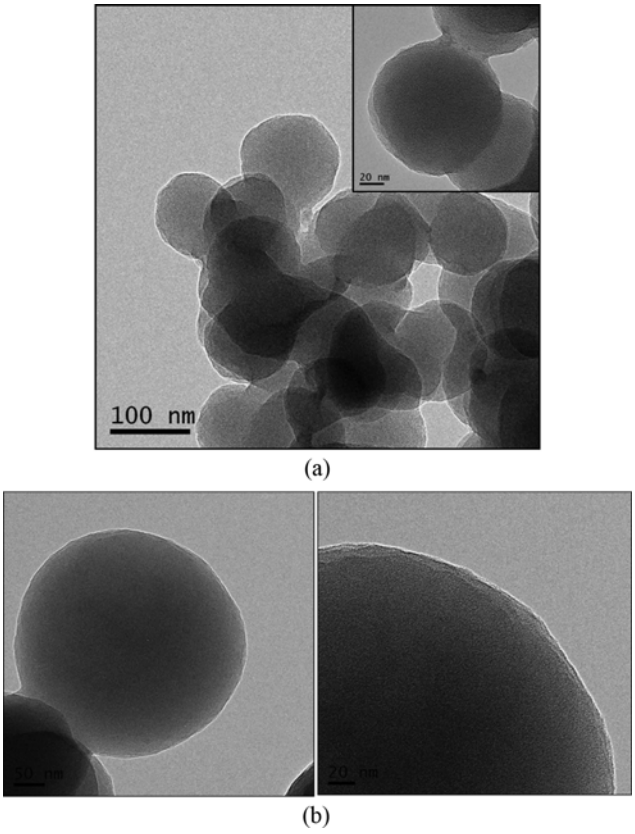

Fig. 2. TEM images of native CNS: (a) CNS1 (reaction temperature: 170 °C, reaction time: 14 h) and (b) CNS2 (reaction temperature: 170 °C, reaction time: 19 h).

RESULTS AND DISCUSSION

1. Characterization of CNS

Fig. 1 shows an SEM image of the native CNS sample. The SEM image reveals nearly spherical shape with larger diameters ranging from 1-3 µm, and small diameters of about hundred to few hundred nm. Small carbon spheres exist in agglomeration form rather than in a uniform individualized form. Fig. 2 presents the TEM image of native CNS1 (reaction time of 14 hrs) and CNS2 (19 hrs) samples. The TEM micrograph reveals that the microspheres are carbonaceous and amorphous.

X-ray diffraction (XRD) patterns of the two CNS samples showed a single broad peak at around 20° (2θ), which corresponds to the typical graphitic (*002*) planes [24]. The interlayer distance of (*002*) planes were 0.465 nm and 0.433 nm for CNS1 and CNS2 respectively (Table 2), which is larger than that of interlayer distance of graphite (d_{002}=0.335 nm). This result agrees with the TEM/SEM results that CNSs are of various sizes and mostly amorphous carbon with some crystalline graphitic carbon [25]. Raman spectrum of CNS shows strong peaks of 1,580 cm^{-1} and a relatively diffuse peak of 1,360 cm^{-1}. The 1,580 cm^{-1} band is attributed to the in-plane vibrations of crystalline graphite and is commonly known as the 'G', or graphite, band. The peak at 1,360 cm^{-1} is due to a vibrational mode associated with graphite edges [26] and is known as the 'D', or disorder, band. Surface area and pore volume from BET analysis confirmed that CNSs are basically nonporous [27]. These structural characteristics of CNS are summarized in Table 2.

Fig. 3 compares the FTIR spectra of native CNS1/CNS2 against their functionalized samples (CNS1-OH/CNS2-OH), respectively. The broad band in the range 3,100-3,400 cm^{-1} is attributed to hydroxyl (-OH) stretching of carboxylic bonds [28]. The band at 1,700 cm^{-1} is due to the stretching vibration of undissociated carbonyl (C=O) groups, and the neighboring band at 1,615 cm^{-1} is attributed to C=C stretching [29-32]. The three peaks found at 1,604, 1,510

Table 2. Characteristics of CNS samples

Samples	EDX-TEM		BET		Interlayer spacing (Å)*	Raman peaks (cm^{-1})	Experimental time (h)
	C (wt%)	O (wt%)	Surface area (m^2/g)	Pore volume (cc/g)			
CNS1	90.4	9.6	8.5	0.007	4.65	~1360, ~1580	14
CNS2	90.8	9.2	17.9	0.02	4.33	1360, ~1580	19

*From XRD 2(θ) data

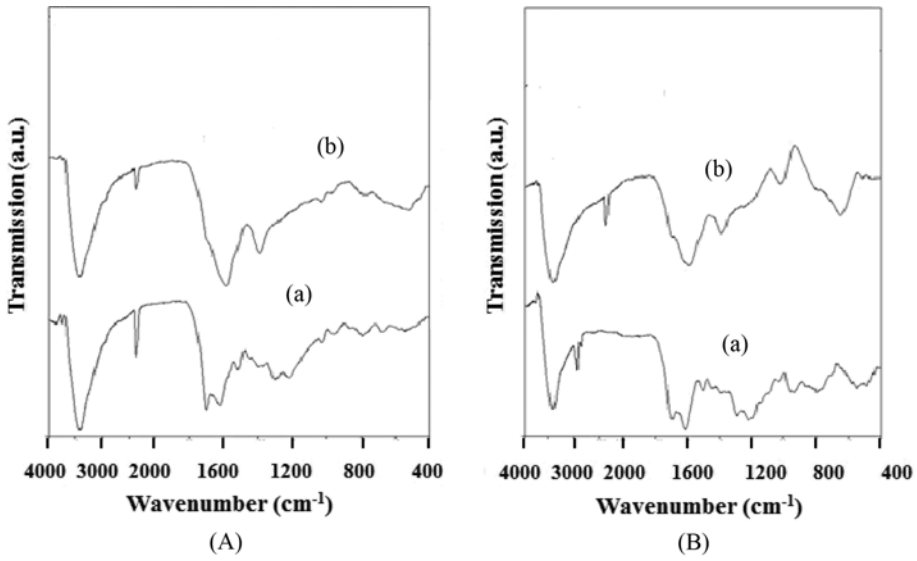

Fig. 3. FTIR spectra of CNS: (A) CNS1 (reaction temperature: 170 °C, reaction time: 14 h): (a) native CNS1 and (b) CNS1-OH (B) CNS2 (reaction temperature: 170 °C, reaction time: 19 h): (a) native CNS2 and (b) CNS2-OH.

and 1,395 cm^{-1} are the result of bond vibrations of five-member heteroaromatic rings with double bonds [25,33-35]. The bands at 1,302 cm^{-1} and 1,023 cm^{-1} correspond to C-OH stretching and OH bending vibrations in C-OH, respectively [22,36]. Fig. 3(a) shows the FTIR spectra of native CNS1, CNS1-OH. CNS1-OH spectra shows almost no peak at 1,700 cm^{-1}, indicating that C=O stretching was greatly reduced. Conversely, the peak at 1,385 cm^{-1} (-COO^-) was noticeably enhanced.

Afkhami et al. [37] suggests that the possible reason for these changes is the following surface reaction occurring to lactone groups.

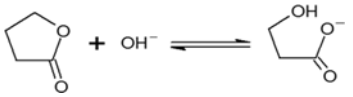

Pendleton et al. [38] suggested the following surface reaction of hydroxyl groups with NaOH also has an effect.

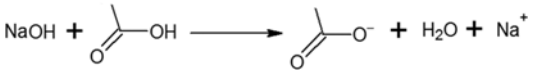

Song et al. [23] reported that treatment with NaOH has no effect on the pore volume, surface area and morphology of CNS. Fig. 3(b) shows the spectra of native CNS2 vs the functionalized CNS2-OH. The C-H asymmetric stretching found at 2,925 cm^{-1} was greatly reduced by the basic treatment. In a similar manner to CNS1, NaOH-treated CNS1-OH had a diminished C=O peak and an increased C=C stretching. Also, the surface-treated CNS had an increase in deprotonated carboxylate groups as well as an increased peak at 1,023 cm^{-1} (OH bending in C-OH).

2. Adsorption Studies

The native CNS1 and CNS2 showed similar adsorption capacity as shown in Fig. 4. As the CNSs are nonporous, the main adsorption mechanisms of metal ions have been attributed to chelation and reduction [39-42]. Fig. 5 shows the adsorption isotherm data (solid circle) and removal efficiency (empty circles) of Cu^{2+}

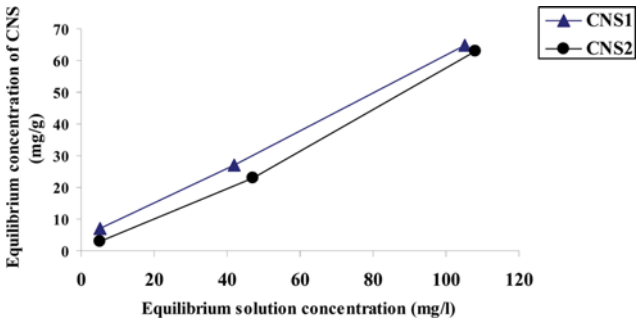

Fig. 4. Cu^{2+} adsorption isotherm of native CNS1 and CNS2 samples (Room temperature, RPM: 250, testing time: 12 h).

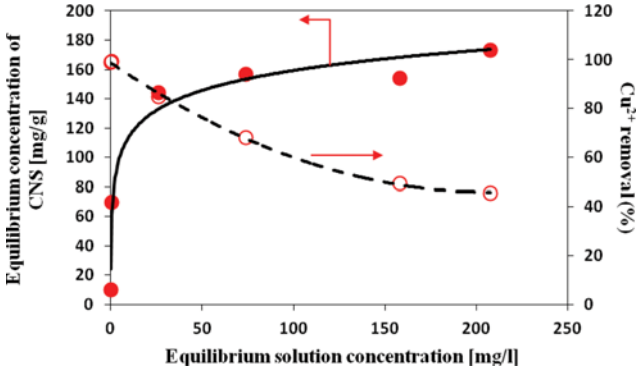

Fig. 5. Cu^{2+} adsorption isotherm and the removal efficiency of the batch system on CNS1-OH (Room temperature, RPM: 250, testing time: 12 h).

on CNS1-OH samples. It is seen that, 1) the adsorption follows a typical type-I isotherm according to IUPAC classification, suggesting a monolayer adsorption on a homogeneous surface; and 2) the efficiency is high at the lower equilibrium concentration (>99% at the first point, of which 25 mg of sample is dosed into 25 mL stock

Table 3. Comparison of adsorption capacities of Cu^{2+} on various adsorbents

Adsorbents	Capacity g-Cu^{2+}/Kg-adsorbent	Ref.
CNS1-OH	~170	This paper
CNS2-OH	~145	This paper
Cellulose pulp	5.0	[43]
Compost	12.8	[43]
Rolling mill scale	40	[44]
Coal	1.6	[45]
Blast furnace sludge	18	[46]
Molecular-imprinted chitosan hydrogel	12	[47]
Ion-exchanged zeolite tuff	26	[48]

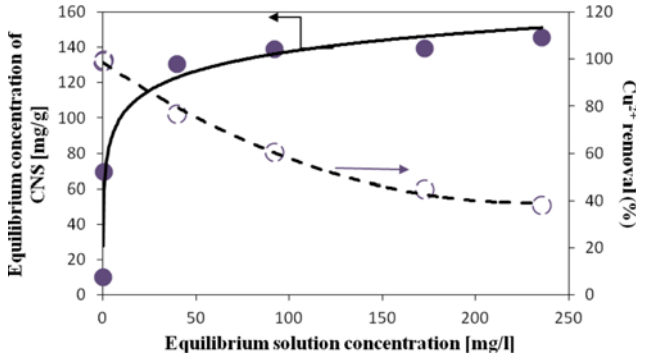

Fig. 6. Cu^{2+} adsorption isotherm and the removal efficiency of the batch system on CNS2-OH (Room temperature, RPM: 250, testing time: 12 h).

solution) and then gradually decreases. The maximum adsorption capacity obtained was 172×10^{-3} Kg Cu^{2+}/Kg-adsorbent, which is higher than most of the well-known adsorbents, as compared in Table 3.

The adsorption isotherm and removal efficiency on CNS2-OH are shown in Fig. 6 as solid circle and dotted circle, respectively, which is similar to the one on CNS1-OH with the main difference being the slightly-lower maximum adsorption capacity.

Fig. 7 compares the fitting goodness of two isotherm models to the experimental data on each hydroxyl functionalized CNS sample. The dashed lines represent the linear plot of Langmuir equation ($(C_e/q_e)=(1/bq_m)+(C_e/q_m)$), while the dotted lines show the linearized Freundlich equation ($\ln q_e=\ln k_f+(1/n)\ln C_e$). In these equations, q_m is the maximum capacity, b and k_f the affinity, and C_e the equilibrium concentration, respectively. We see that the Langmuir isotherm fitted all the data well (R^2>0.96 on each CNS). The adsorption capacity of CNS2-OH is lower than that of CNS1-OH, suggesting that the CNS with more regular graphite content (or longer reaction time) presents no advantage for this application. A possible reason is that a more graphitized CNS contains less functional groups and unsaturated bonds on its surface. On the other hand, the Freundlich isotherm gave slightly inferior fittings (R^2< 0.95) on each -OH functionalized CNS, suggesting that its underlining mechanisms (a heterogeneous surface) differ from our system [10]. Langmuir model states that the adsorption is monolayered, a homogeneous surface and with no interaction among the adsorbed species [42], which are more consistent with our adsorption system in which the redox process played a major role in the adsorption process [19,23,42]

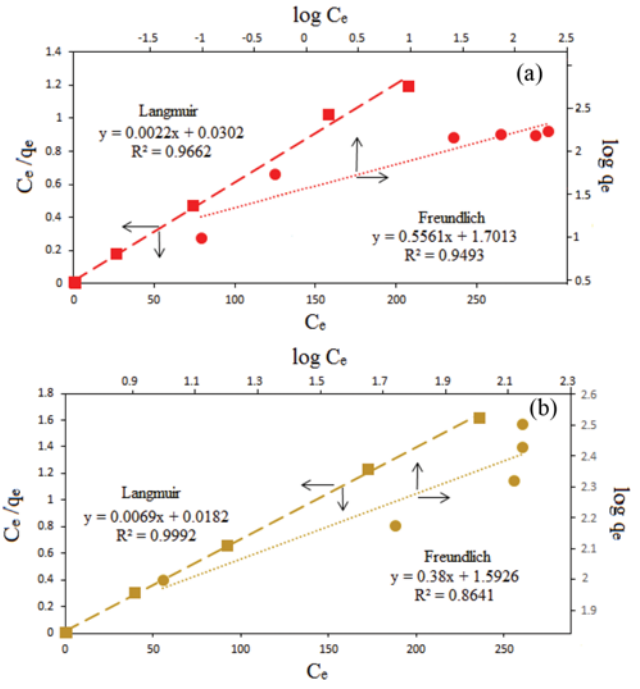

Fig. 7. Fittings of linearized Langmuir and Freundlich isotherm models for Cu^{2+} ion removal on CNS samples; (a) CNS1-OH; (b) CNS2-OH.

The theoretical maximum adsorption capacity predicted by the Langmuir equation for CNS2-OH is 144.9 mg Cu^{2+}/g, which is very close to the experimentally determined value of 145.5 mg Cu^{2+}/g-adsorbent. Also, a nearly perfect correlation coefficient of >0.99 and an acceptable R_L value of 0.007 of CNS2-OH was obtained. Comparing the overall CNS1 and CNS2 results reveals that CNS1 is a better ad- sorbent for Cu^{2+} ions removal. Therefore, the CNS with a shorter reaction time and a lower amorphous content resulted in a higher Cu^{2+} adsorption capacity.

CONCLUSIONS

Colloidal carbon microspheres were synthesized from a glucose solution by using hydrothermal synthesis process and were used to remove copper ions from aqueous solutions which resemble the refinery effluents. Increasing the reaction time resulted in CNS with a slightly orderly structure as revealed by XRD patterns and TEM. N_2 adsorption-desorption isotherm confirmed that CNSs are nonporous and contain low surface area (<20 m^2/g). The adsorption of metal ions on CNS samples is mainly a chemisorption process and surface activation with hydroxyl groups greatly enhanced the adsorption capacity. The adsorption isotherms are better fitted by the Langmuir model. The more amorphous sample from a shorter reaction time had a higher adsorption capacity of ~170×10^{-3} Kg Cu^{2+}/Kg-adsorbent. This study revealed that sur-

face activated CNS is a promising adsorbent for the removal of heavy metals for an example Cu^{2+} from effluents of chemical/petroleum industries.

REFERENCES

1. A. Agrawal, K. K. Sahu and B. D. Pandey, *AIChE J.*, **50**, 2430 (2004).
2. S. Cay, A. Uyanik and A. Ozasik, *Sep. Purif. Technol.*, **38**, 273 (2004).
3. B. Bayat, *J. Hazard. Mater.*, **95**, 251 (2002).
4. T. M. Alslaibi, I. Abustan, M. A. Ahmad and A. Abu Foul, *Desalination Water Treatment*, **52**, 7887 (2014).
5. D. M. Araujo, M. I. Yoshida, F. Stapelfeldt, C. F. Carvalho, C. L. Donnici and G. F. Kastner, *Rem-Revista Escola De Minas*, **62**, 463 (2009).
6. S. Biniak, M. Pakula, G. S. Szymanski and A. Swiatkowski, *Langmuir*, **15**, 6117 (1999).
7. J. P. Chen and S. Wu, *J. Colloid Interface Sci.*, **280**, 334 (2004).
8. J. P. Chen, S. N. Wu and K. H. Chong, *Carbon*, **41**, 1979 (2003).
9. X. C. Chen, G. C. Chen, L. G. Chen, Y. X. Chen, J. Lehmann, M. B. McBride and A. G. Hay, *Bioresour. Technol.*, **102**, 8877 (2011).
10. Z. Z. Chowdhury, S. M. Zain, R. A. Khan and M. S. Islam, *Korean J. Chem. Eng.*, **29**, 1187 (2012).
11. R. P. Han, L. J. Zhang, C. Song, M. M. Zhang and H. M. Zhu, *Carbohydr. Polym.*, **79**, 1140 (2010).
12. H. Aydın, Y. Bulut and Ç. Yerlikaya, *J. Environ. Manage.*, **87**, 37 (2008).
13. H. Demiral and C. Güngör, *J. Cleaner Production*, **124**, 103 (2016).
14. U. Divrikli, A. A. Kartal, M. Soylak and L. Elci, *J. Hazard. Mater.*, **145**, 459 (2007).
15. Y. F. Jia, C. J. Steele, I. P. Hayward and K. M. Thomas, *Carbon*, **36**, 1299 (1998).
16. M. L. Cantuaria, A. F. D. Neto, E. S. Nascimento and M. G. A. Vieira, *J. Cleaner Production*, **112**, 1112 (2016).
17. D. Ozdes, A. Gundogdu, B. Kemer, C. Duran, H. B. Senturk and M. Soylak, *J. Hazard. Mater.*, **166**, 1480 (2009).
18. M. Tuzen and M. Soylak, *J. Hazard. Mater.*, **164**, 1428 (2009).
19. X. Song, Y. Wang, K. Wang and R. Xu, *Ind. Eng. Chem. Res.*, **51**, 13438 (2012).
20. L. Frusteri, C. Cannilla, G. Bonura, A. L. Chuvilin, S. Perathoner, G. Centi and F. Frusteri, *Catal. Today*, **277**, 68 (2016).
21. L. Frusteri, C. Cannilla, K. Barbera, S. Perathoner, G. Centi and F. Frusteri, *Carbon*, **59**, 296 (2013).
22. X. Sun, X. M. Sun and Y. D. Li, *Angewandte Chemie (International ed.)*, **43**, 597 (2004).
23. X. Song, P. Gunawan, R. Jiang, S. S. J. Leong, K. Wang and R. Xu, *J. Hazard. Mater.*, **194**, 162 (2011).
24. K. Wang. S. Mondal and A. T. Derebe, *J. Chem. Eng. Res. Updates*, **1**, 35 (2014).
25. N. Puvvada, B. P. Kumar, S. Konar, H. Kalita, M. Mandal and A. Pathak, *Sci. Technol. Adv. Mater.*, **13**, 045008 (2012).
26. A. Ilie, C. Durkan, W. I. Milne and M. E. Welland, *Phys. Review B*, **66**, 045412 (2002).
27. D. D. Do, *Adsorption analysis: Equilibria and kinetics*, Imperial College Press (1998).
28. N. B. Colthup, L. H. Daly and S. E. Wiberley, Introduction to infrared and Raman spectroscopy, Elsevier (1990).
29. I. Novák, P. Sysel, J. Zemek, M. Špírková, D. Velič, M. Aranyosiová, Š. Florián, V. Pollák, A. Kleinová, F. Lednický and I. Janigová, *European Polym. J.*, **45**, 57 (2009).
30. S. Xuguang, *Spectrochim. Acta Part A: Mole. Biomolecular Spectroscopy*, **62**, 557 (2005).
31. C. Yao, Y. Shin, L.-Q. Wang, C. F. Windisch, W. D. Samuels, B. W. Arey, C. Wang, W. M. Risen and G. J. Exarhos, *J. Phys. Chem. C*, **111**, 15141 (2007).
32. S. Shin, J. Jang, S. H. Yoon and I. Mochida, *Carbon*, **35**, 1739 (1997).
33. J. A. Joule and K. Mills, Heterocyclic Chemistry, Wiley (2010).
34. I. Atamanenko, A. Kryvoruchko, L. Yurlova and E. Tsapiuk, *Desalination*, **147**, 257 (2002).
35. X.-h. Guan, G.-h. Chen and C. Shang, *J. Environ. Sci.*, **19**, 438 (2007).
36. R. Demir-Cakan, N. Baccile, M. Antonietti and M.-M. Titirici, *Chem. Mater.*, **21**, 484 (2009).
37. A. Afkhami, T. Madrakian, Z. Karimi and A. Amini, *Colloids Surf., A: Physicochem. Eng. Aspects*, **304**, 36 (2007).
38. P. Pendleton, S. H. Wu and A. Badalyan, *J. Colloid Interface Sci.*, **246**, 235 (2002).
39. J. Wang, X. Yin, W. Tang and H. Ma, *Korean J. Chem. Eng.*, **32**, 1889 (2015).
40. M. A. Barakat, *Arabian J. Chem.*, **4**, 361 (2011).
41. X. B. Wang, J. Liu and W. Z. Xu, *Colloids Surf., A-Physicochem. Eng. Aspects*, **415**, 288 (2012).
42. V. C. G. Dos Santos, J. De Souza, C. R. T. Tarley, J. Caetano and D. C. Dragunski, *Water Air and Soil Pollution*, **216**, 351 (2011).
43. M. Ulmanu, E. Marañón, Y. Fernández, L. Castrillón, I. Anger and D. Dumitriu, *Water, Air, & Soil Pollution*, **142**, 357 (2003).
44. F. Lopez, M. Martın, C. Perez, A. Lopez-Delgado and F. Alguacil, *Water Res.*, **37**, 3883 (2003).
45. S. Karabulut, A. Karabakan, A. Denizli and Y. Yürüm, *Sep. Purif. Technol.*, **18**, 177 (2000).
46. A. Lopez-Delgado, C. Perez and F. Lopez, *Water Res.*, **32**, 989 (1998).
47. X. Song, C. Li, R. Xu and K. Wang, *Ind. Eng. Chem. Res.*, **51**, 11261 (2012).
48. J. Perić, M. Trgo and N. V. Medvidović, *Water Res.*, **38**, 1893 (2004).